



Reuse of coal combustion ashes as alternatives to cement and natural fine aggregate in green building bricks production for sustainable development

Article info

Type of article:

Original research paper

DOI:

<https://doi.org/10.58845/jstt.utt.2025.en.5.3.126-144>

*Corresponding author:

Email address:

htphuoc@ctu.edu.vn

Received: 06/05/2025

Received in Revised Form:
15/09/2025

Accepted: 28/09/2025

Van-Dung Nguyen¹, Trinh Thi Ha Phuong¹, Lanh Si Ho², Trong-Phuoc Huynh^{3*}

¹Faculty of Engineering, Technology, and Communication, Hong Duc University, No. 565, Quang Trung Street, Hac Thanh Ward, Thanh Hoa City, Vietnam.

²Department of Geotechnical Engineering and Metro, University of Transport Technology, Ha Noi City, Vietnam.

³Faculty of Civil Engineering, College of Engineering, Can Tho University, Campus II, 3/2 Street, Ninh Kieu Ward, Can Tho City, Vietnam.

Abstract: The coal thermal power plant generates a lot of ashes, including fly ash (FA) and bottom ash (BA), which potentially pollute the environment. Thus, to promote sustainable development, this research assesses the feasibility of converting these ashes into green building bricks (GB). In detail, BA was utilized to fully replace natural fine aggregate in the GB mixes, and FA was utilized as a binder material to partially replace cement at various weight percentages of 0%, 30%, 50%, 70%, and 85%. The designed grade of GB in this study is M7.5, as classified in the TCVN 6477:2016, which is commonly used in non-loading bearing wall applications. The influence of FA replacement level on the GB's properties, such as compressive strength, ultrasonic pulse velocity (UPV), electrical resistance (ER), and thermal conductivity (TC), was investigated. Moreover, the mineralogy change and microstructure of the GB samples were identified using X-ray diffraction and scanning electron microscopy techniques. The experimental findings demonstrate that replacing cement with FA had a substantial effect on all of the GB sample performance. At 28 days, GB samples had compressive strength, UPV, ER, and TC values ranging from 3.1 to 14.8 MPa, 1526 to 3360 m/s, 5.1 to 18.3 kΩ.cm, and 0.29 to 0.69 W/mK, respectively. These findings illustrate the viability of employing FA and BA in the manufacturing of GB for sustainable construction. As a result, the GB with ≤30% FA replacement met the target strength of ≥7.5 MPa, qualifying for use in a non-loading bearing wall in real practice.

Keywords: Green building brick; coal combustion ash; fly ash; bottom ash; microstructure.

1. Introduction

The construction industry is one of the largest sectors contributing to global economic growth, yet it also has a significant environmental

impact, especially concerning resource depletion and waste generation. One of the most critical issues in modern construction is the environmental footprint of building materials, particularly cement

and natural aggregates. Cement production is responsible for approximately 9.5% of global carbon dioxide emissions, making it one of the major contributors to climate change [1–3]. Additionally, the extraction of natural aggregates for use in concrete leads to the depletion of natural resources and poses environmental challenges, such as habitat destruction and water table depletion [4].

In response to these environmental challenges, the concept of sustainable construction has gained prominence, with efforts focusing on reducing the carbon footprint of construction materials through alternative binders and aggregates [5–7]. The reuse of industrial by-products, such as coal combustion ashes, has emerged as a promising solution for enhancing sustainability in the construction sector. Coal thermal power plants produce vast quantities of fly ash (FA) and bottom ash (BA) as by-products of coal combustion. A large amount of these wastes is available in Vietnam [7, 8]. These ashes are annually released in approximately 25 million tons and are expected to be 40 million tons by 2030 [7, 9], whereas the amount of BA accounts for around 20-25% of the total amount of FA and BA. While these ashes have traditionally been disposed of in landfills, their high silica content and pozzolanic properties make them potential candidates for use in construction materials [6, 10–12].

The use of industrial by-products as replacements for cement and natural fine aggregates has been widely investigated due to their potential to enhance sustainability in construction. FA has been extensively studied for its pozzolanic properties, allowing it to partially replace cement in concrete mixes, improving workability and durability, and reducing carbon emissions associated with cement production [13]. Similarly, BA has been explored as a fine aggregate replacement, with studies showing that while BA may reduce compressive strength when used alone, its performance improves when combined with FA, indicating a synergistic effect

between these materials [7, 14]. Bian et al. [15] highlighted the variability in BA's performance depending on mix design and its content, while Chee [16] reviewed the environmental benefits of using FA in mortar. Together, these findings underscore the promising role of FA and BA in green building materials, offering a sustainable solution for reducing the environmental impact of coal-fired power plants while conserving natural resources.

In Vietnam, using unburnt bricks to replace traditional fired bricks is a modern and inevitable trend in the construction materials manufacturing industry [17]. Many documents of the Departments and Branches have been issued to promote the development of unburnt construction materials [18–21], the Prime Minister has approved the Program for the development of unburnt construction materials until 2020 in Decision No. 567/QĐ-TTg dated April 28, 2010; Directive No. 10/CT-TTg dated April 16, 2012 on increasing the use of unburnt construction materials, limiting the production and use of fired clay bricks; and most recently, Decree 24a/2016/NĐ-CP dated April 5, 2016 of the Government on the management of construction materials; In which, encouraging the development of unburnt construction materials, Circular 13/2017/TT-BXD regulates the use of unburnt construction materials in construction works, effective from February 1, 2018, replacing Circular 09/2012/TT-BXD. Recent research has increasingly concentrated on the creation of eco-friendly bricks by utilizing industrial by-products, seeking to reduce the environmental footprint of conventional brick manufacturing. Irfan-ul-Hassan et al. [22] showed that red mud, a waste material from alumina production, when combined with FA, results in green building bricks (GB) that exhibit improved mechanical properties, reduced CO₂ emissions, and lower production costs compared to traditional bricks. Similarly, Wang et al. [23] investigated the incorporation of recycled aggregates and waste glass into permeable bricks, fine-tuning the porosity to enhance water

absorption and freeze-thaw resistance. Jothilingam et al. [24] leveraged tannery sludge along with FA and ground granulated blast-furnace slag (GGBFS) to formulate sustainable GB, achieving notable gains in strength while minimizing environmental damage. Nikvar-Hassani et al. [25] explored the use of copper mine tailings for geopolymer bricks, demonstrating that the inclusion of GGBFS as a supplementary material accelerates geopolymerization and improves mechanical properties. Additionally, Cai et al. [26] assessed the feasibility of quarry sludge as a siliceous material in autoclaved bricks, showing that optimal curing conditions and an appropriate Ca/Si ratio result in better strength and durability. Iftikhar et al. [27] developed geopolymer-based green clay bricks, optimizing the proportion of clay and FA, which resulted in bricks with superior performance and a smaller environmental footprint compared to conventional fired clay options. Taken together, these studies highlight the potential of utilizing waste-derived materials to produce sustainable, high-performance building materials, contributing to waste reduction and promoting eco-friendly construction practices.

The potential to replace both cement and natural fine aggregates with coal combustion ashes in the production of GB offers an innovative solution to the pressing need for sustainable alternatives in construction. Several studies have investigated the use of FA as a partial replacement for cement in concrete [2, 7], but the incorporation of both FA and BA in GB is still an underexplored area. Moreover, the effects of varying FA replacement levels on the mechanical, physical, and microstructural properties of the bricks remain inadequately understood. Incorporating FA and BA into the production of GB not only helps in reducing the environmental impact of coal combustion but also addresses the growing demand for sustainable construction materials.

This research aims to explore the feasibility of utilizing FA and BA in the production of GB. Specifically, the study investigates the influence of

replacing cement with FA at various levels (0%, 30%, 50%, 70%, and 85%) and using BA as a fine aggregate. The study evaluates the performance of the resulting GB samples in terms of compressive strength (CS), ultrasonic pulse velocity (UPV), electrical resistance (ER), and thermal conductivity (TC). Additionally, the microstructure and mineralogy of the GB are analyzed using X-ray diffraction (XRD) and scanning electron microscopy (SEM) techniques to understand the interaction between the components at a microscopic level. The results of this research provide valuable insights into the potential of coal combustion ashes as sustainable materials for the construction industry and contribute to the development of greener, more environmentally friendly building products.

2. Material properties and experimental details

2.1. Material properties

The starting materials employed in this investigation included grade-40 Portland cement, type-F FA, and BA, with blended cement-FA and BA serving as a binder and fine aggregate, respectively. The FA and BA in this study were sourced from an ordinary coal-fired power plant using pulverized combustion technology (Nghi Son thermal power plant). The specific gravity of cement and FA was 3.12 and 2.16, respectively. BA, on the other hand, had a density of 1987 kg/m³, a high water capacity of 23.2%, a fineness modulus of 1.97, and a particle size distribution as displayed in Fig. 1.

The strength activity index compared to cement of FA was 86%. The primary chemical compositions of these GB components are listed in Table 1. As shown in Table 1, both FA and BA have a high value of LOI. These high values of LOI may be caused by unburnt impurities, as indicated in the previous studies [28–30]. Although containing high LOI, the characteristics of coal ashes from the Nghi Son thermal power plant did not cause significant health and environmental risks, as reported and used in many prior studies [31–35].

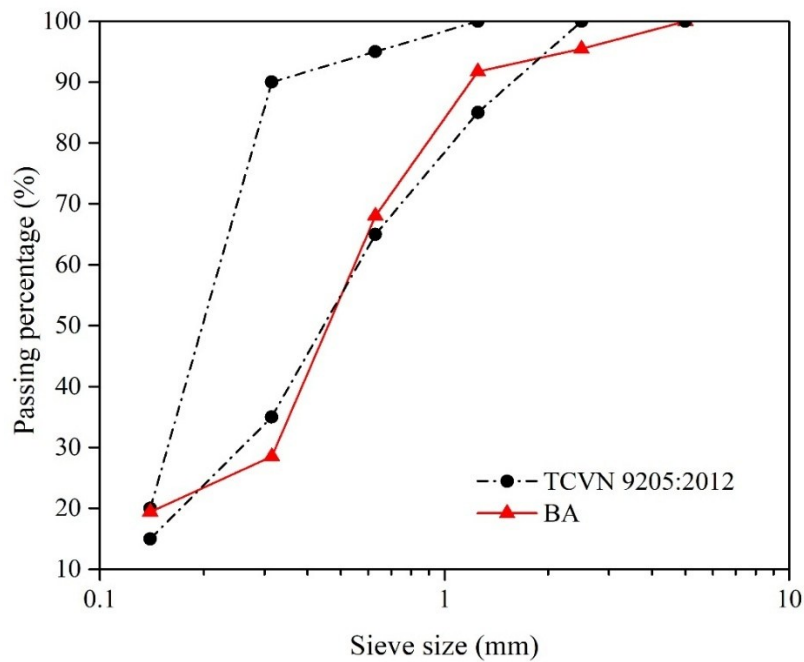


Fig. 1. Particle size distribution of BA

Table 1. Chemical compositions of starting materials

Elements	Cement (wt.%)	FA (wt.%)	BA (wt.%)
SiO ₂	21.2	51.5	52.2
Al ₂ O ₃	5.5	20.2	20.0
Fe ₂ O ₃	4.9	7.1	7.2
CaO	61.0	2.0	2.4
MgO	3.0	1.2	1.2
SO ₃	1.5	-	-
K ₂ O	0.5	-	-
Other	2.0	2.2	2.0
Loss on ignition	0.4	15.0	15.9

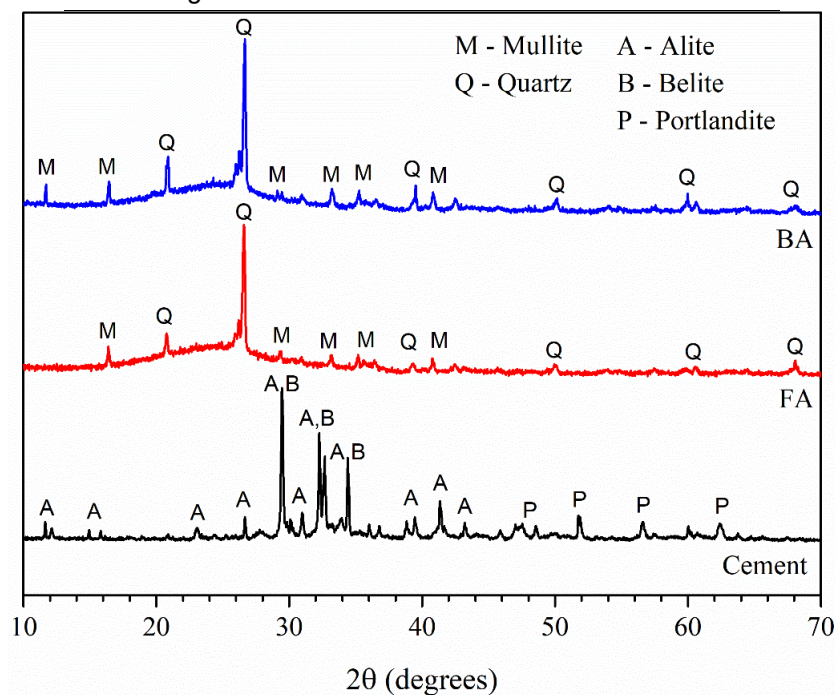


Fig. 2. XRD patterns of starting materials

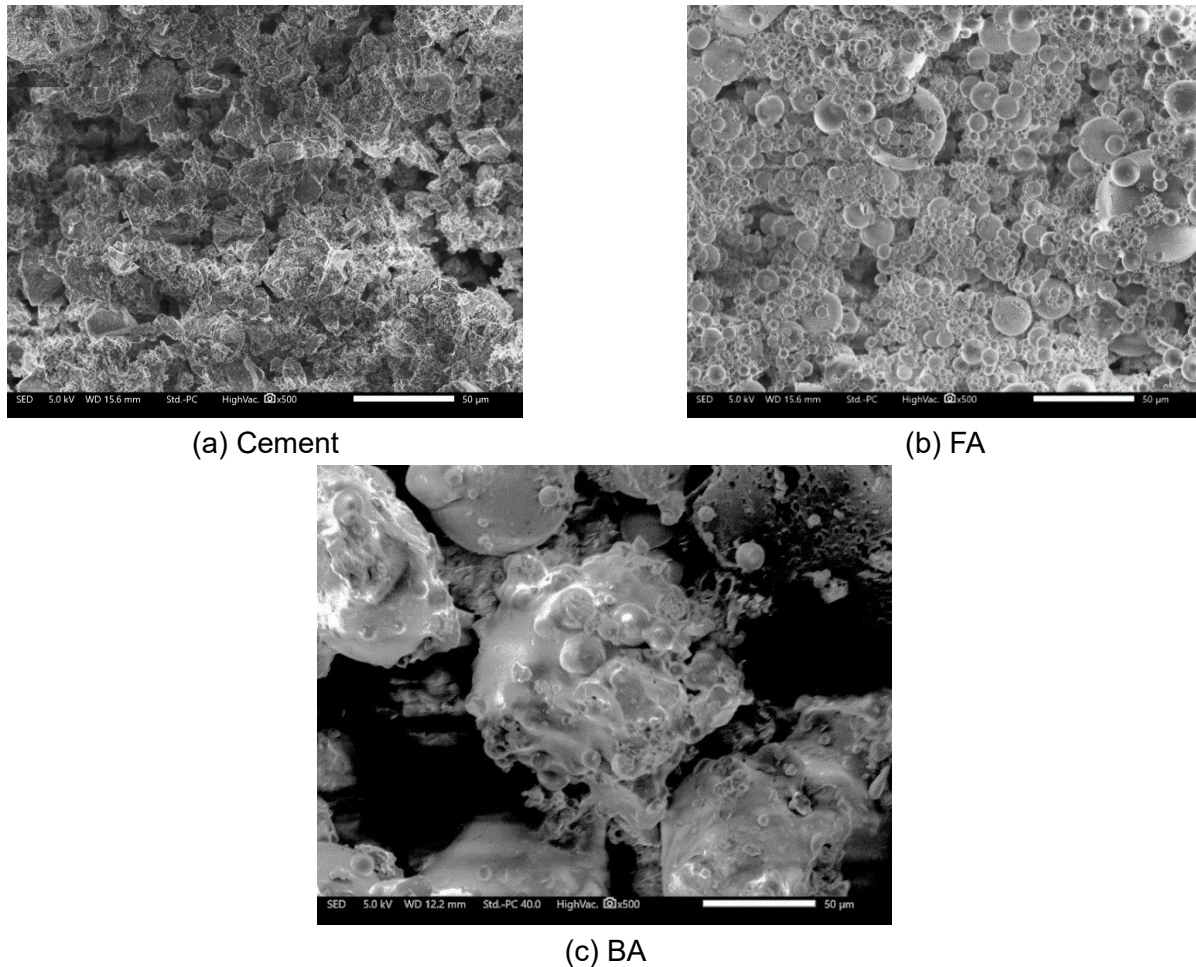


Fig. 3. SEM images of starting materials

Figs. 2 and 3 show the raw materials' XRD patterns and SEM morphologies. It can be seen that SiO_2 , which is mostly crystalline, was a key component of the starting materials. Besides, both FA and BA included a high percentage of Al_2O_3 , while cement contained a high amount of CaO . Furthermore, Fig. 3 reveals that FA was made up of spherical and smooth particles of varying sizes. The shape of BA particles was similar to that of FA particles, but BA particles were larger and had a porous structure. Whereas cement consisted primarily of irregularly shaped particles

2.2. Mixture proportions

The designed grade of GB in this study is M7.5 as classified in the TCVN 6477:2016 [36]. The primary goal of this study is to investigate the reuse of low-quality coal combustion FA and BA as starting materials for making GB. In detail, BA was used as fine aggregate and FA was used to partially replace cement in the GB mixtures at various levels

of 0%, 30%, 50%, 70%, and 85% by weight to evaluate the impacts of FA content on the performance of GB samples. For all GB mixtures (Table 2), a fixed w/b ratio of 0.4 was used. It is noted that the designed parameters were chosen according to the preliminary trials in the laboratory with proper adjustments.

2.3. Sample preparation and test methods

Based on the estimated combinations in Table 2, every material was precisely prepared and measured before being mixed in the laboratory using a free mechanical mixer. The steps involved in preparing GB samples are detailed in Fig. 4. Cement, FA, and BA were first dry-mixed for two minutes. To achieve a uniform mixture, the mixer was then filled with the mixing water, and the mixing process was maintained for three more minutes. Following mixing, a steel mold of $160 \times 85 \times 40$ mm was used to make the GB samples, each of which was formed at a constant 0.5 MPa forming

pressure. After forming, the completed GB samples were promptly demolded and kept at room temperature until the designed testing time.

To evaluate the GB's performance, the GB samples were examined for CS, UPV, ER, and TC following the relevant Vietnamese Standards and technical guidelines for construction materials. In detail, the CS (using a 50-C34C02 automatic compression tester of CONTROLS, Italy) and UPV (using a C369N ultrasonic pulse velocity tester of MATEST, Italy) were tested at 3, 7, 14, and 28 days in accordance with TCVN 6477:2016 [36] and TCVN 9357:2012 [37], respectively. The 28-day ER and TC of the GB samples were directly measured

using a four-point Wenner array (Resipod resistivity meter of PROCEQ, Switzerland) [38] and a portable device model of ISOMET-2014 (Slovakia) [28], respectively. For each test method, three samples were tested at each testing age, and the average value was reported to ensure the reliability of the results.

The microstructure of the GB samples at 28 days was also characterized using the XRD (step scan of 0.02 and 2θ angle of $10\text{--}70^\circ$) and SEM (using 5 kV and 25 pA chamber pressure) techniques [12]. SEM and XRD analyses provided insights into the microstructure and mineralogical composition of the GB samples.

Table 2. Material proportions of GB mixtures

Mix ID.	FA content (%)	Material proportions (unit: kg)			
		Cement	FA	BA	Water
MFA00	0	320	0	1531	128
MFA30	30	224	96	1531	128
MFA50	50	160	160	1531	128
MFA70	70	96	224	1531	128
MFA85	85	48	272	1531	128

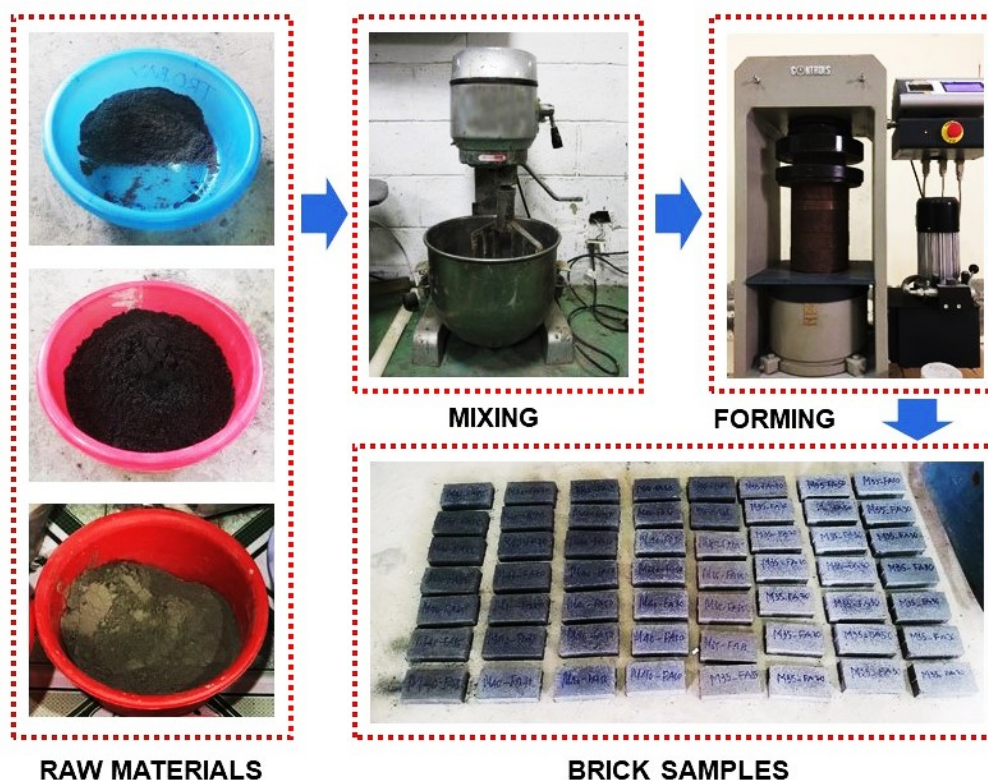


Fig. 4. Procedures for GB preparation

3. Results and discussion

3.1. Compressive strength

The CS of the GB samples (Fig. 5) showed

distinct patterns depending on the FA content in the mixture, with increasing FA percentages leading to a decrease in early-stage strength. At day 3, the

control mix (MFA00, 0% FA) exhibited the highest CS of 8.2 MPa. When compared to the MFA30 mix (30% FA), the CS dropped by approximately 34.5%, from 8.2 MPa (MFA00) to 5.41 MPa. This drop highlights the initial effect of FA replacement, where FA's slower pozzolanic reaction reduces the early-strength development typical of pure cement.

By day 28, the control mix (MFA00) reached 14.82 MPa, while the MFA30 mix (30% FA) had a CS of 10.15 MPa, showing a reduction of around 31.5% compared to the MFA00 mix. This percentage reduction illustrates that even though FA contributes to long-term strength, the early strength is significantly compromised. The strength development of the MFA30 mix suggests that 30% FA replacement provides a good balance between sustainability and sufficient early performance. The mix with 50% FA replacement (MFA50) experienced a more pronounced reduction in CS. At day 3, MFA50 showed a CS of 2.57 MPa, which is 68.7% lower than the control mix (MFA00). By day 28, the CS of MFA50 reached 6.92 MPa, a

53.3% reduction compared to the MFA00 mix. This dramatic decrease in early strength, particularly at day 3, is attributed to the higher FA content, which delays the pozzolanic reactions and reduces the cement content responsible for early strength development. Although the long-term strength of MFA50 increases, its early-age performance remains significantly lower compared to the control mix. The impact of further increasing FA content to 70% and 85% (MFA70 and MFA85) is even more significant. The CS values at day 3 for MFA70 and MFA85 were 1.53 MPa and 0.77 MPa, respectively, reflecting reductions of 81.3% and 90.6% compared to MFA00. At day 28, the CS for these mixes increased to 5.88 MPa (MFA70) and 3.1 MPa (MFA85), but these still represent reductions of 60.4% and 79.1%, respectively, compared to the control mix (MFA00). These significant reductions in strength at both early and later stages highlight the limitations of using high levels of FA as a replacement for cement, especially when early strength is required.

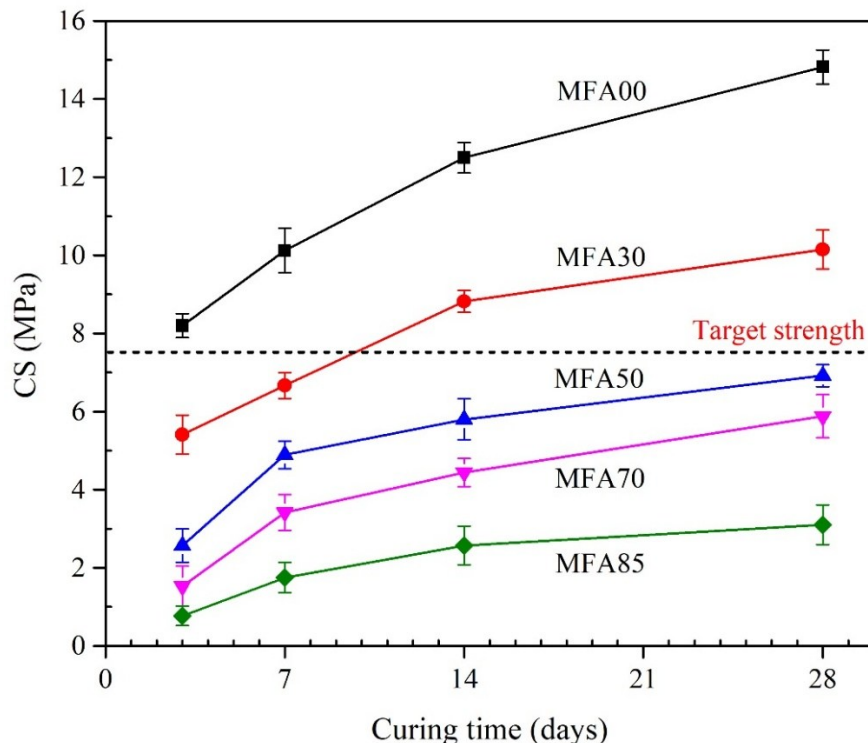


Fig. 5. CS of GB samples

The observed trends are consistent with previous research on the use of FA in construction materials. Adamu et al. [13] reported similar

findings where higher FA content resulted in reduced early CS but enhanced long-term durability due to the continued pozzolanic

reactions. The reduction in strength at higher FA levels is primarily due to the lower reactivity of FA in comparison to cement, leading to slower initial hydration and reduced early-stage strength development.

In short, while the inclusion of FA in the mix provides significant environmental benefits, including reduced carbon footprint and the reuse of industrial by-products, the trade-off in terms of early CS is substantial, especially at higher replacement levels. The MFA30 mix (30% FA) provided the best compromise, with only a 31.5% reduction in CS at 28 days compared to the control mix, making it suitable for applications where moderate early strength is acceptable. In other words, the strength result of this study shows that the GB with $\leq 30\%$ FA replacement met the target strength of ≥ 7.5 MPa, qualifying for use in a non-loading bearing wall in real practice. As the FA content increases to 50% and beyond, the strength reductions become more pronounced, particularly in the early stages. These results suggest that higher FA contents (50–85%) may be more

appropriate for other uses where long-term durability is prioritized over early-stage performance.

3.2. Ultrasonic pulse velocity

The UPV values for the GB samples showed a clear trend of decreasing velocity with increasing FA content, indicating that higher FA replacement leads to a decrease in material density and internal quality (see Fig. 6). At day 3, the MFA00 mix (0% FA) exhibited a UPV of 2901 m/s, which is the highest among all mixes. In comparison, the MFA30 mix (30% FA) recorded a UPV of 2196 m/s, representing a reduction of approximately 24.4%. Similarly, the UPV for MFA50, MFA70, and MFA85 mixes at day 3 were 1932 m/s, 1504 m/s, and 1179 m/s, respectively, indicating decreases of 33.4%, 48.1%, and 59.3% compared to MFA00. These reductions in UPV suggest that the inclusion of FA, particularly in higher amounts, leads to a less dense internal structure, likely due to the slower pozzolanic reactions that reduce the material's uniformity and compactness during early curing.

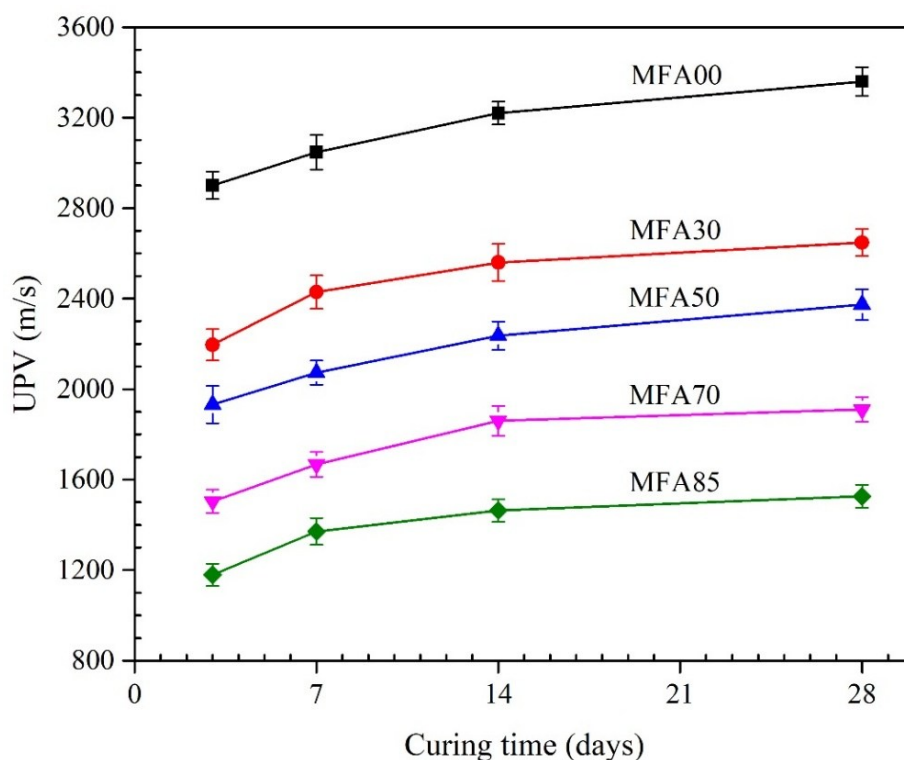


Fig. 6. UPV of GB samples

By day 7, the UPV values for all mixes showed improvement, as expected with continued

curing, with the control mix (MFA00) reaching a UPV of 3047 m/s, a 5% increase compared to day

3. The MFA30 mix improved to 2429 m/s, a 10.6% increase from day 3, and the other mixes followed similar patterns, with the MFA50, MFA70, and MFA85 mixes achieving UPV values of 2073 m/s, 1667 m/s, and 1371 m/s, respectively. These results reinforce the concept that FA contributes positively to the long-term performance of GB samples, as the pozzolanic reactions gain strength over time and lead to a more cohesive microstructure. However, the reduction in UPV is more pronounced in the higher FA content mixes, confirming that the early hydration of cement plays a critical role in enhancing the material's internal density and quality. At 14 and 28 days, the UPV values continued to increase for all mixes, with MFA00 reaching 3220 m/s and 3360 m/s, respectively, indicating continuous hydration and a denser material structure. The MFA30 mix, although still significantly lower than the control mix, showed a gradual improvement, reaching 2560 m/s at day 14 and 2648 m/s at day 28. The MFA50 mix increased from 2237 m/s at day 14 to 2374 m/s at day 28, while the higher FA mixes (MFA70 and MFA85) showed lower values, with MFA70 reaching 1910 m/s and MFA85 reaching 1526 m/s at day 28. The continuous improvement of UPV values over time, albeit slower for mixes with higher FA content, highlights the effectiveness of FA as a sustainable binder, albeit with slower early-stage performance. The relationship between FA content and UPV values is consistent with findings from previous studies. High FA replacement levels reduce the overall density and internal cohesion of the material in the early stages, as reported by Du et al. [39], who found that the presence of FA leads to a more porous and less dense microstructure compared to conventional cement. However, as the curing period extends, the pozzolanic reactions of FA contribute to the densification and strengthening of the material, leading to gradual improvements in UPV values.

In conclusion, the UPV results confirm the observed trend that increasing FA content leads to reduced early-stage material quality, as evidenced

by the lower UPV values at all curing times. However, the long-term performance of FA-based GB is still positive, with continuous increases in UPV as curing progresses. The MFA30 mix (30% FA) provided a relatively balanced performance, showing a 9% reduction in UPV at 28 days compared to the control mix. At higher FA contents (50%, 70%, and 85%), the reduction in UPV becomes more pronounced, particularly in the early stages, indicating that while FA enhances sustainability, its higher replacement levels compromise both early and long-term material uniformity.

The correlation between UPV and CS was evaluated to explore the relationship between the internal quality and structural integrity of the GB samples. The results, as shown in Fig. 7, clearly demonstrate a strong positive linear correlation between UPV and CS, with a high correlation coefficient ($R^2 = 0.962$). This high value of R^2 indicates that the variation in CS is strongly related to changes in UPV, suggesting that as the compressive strength of the GB samples increases, so does the velocity at which ultrasonic pulses travel through the material. This positive correlation aligns with the general understanding that both UPV and CS are indicators of the density and structural integrity of concrete and masonry materials. Higher CS values typically correspond to denser, more solid materials, which allow ultrasonic waves to travel faster. The increased UPV values reflect enhanced uniformity and compactness of the material, which are associated with stronger (higher CS) and more durable bricks. These results align with those of Chen et al. [40], who observed similar correlations between UPV and CS in concrete mixes containing FA. As the FA content increases, the lower CS values in the GB bricks lead to reduced UPV, confirming that the slower pozzolanic reactions of FA compared to cement negatively affect both early strength and overall material density. For instance, the MFA00 mix (0% FA) exhibited the highest CS (14.82 MPa) and UPV (3360 m/s) at 28 days. The MFA30 mix

(30% FA) had a CS of 10.15 MPa and an UPV of approximately 2648 m/s, showing a decrease of around 31.5% in CS and 21.3% in UPV when compared to MFA00. As the FA content increased further, the CS and UPV values for the MFA50, MFA70, and MFA85 mixes progressively decreased, with MFA85 (85% FA) showing a CS of only 3.1 MPa and an UPV of 1526 m/s at 28 days. This represents a decrease of 79.1% in CS and 54.5% in UPV compared to the control mix (MFA00). These results reinforce the conclusion that higher FA content results in lower material density and strength, which, in turn, reduces both CS and UPV.

In practical terms, this strong correlation

between UPV and CS is valuable for non-destructive quality assessment in the field. The high correlation coefficient suggests that UPV measurements could be reliably used to estimate the CS of GB in real-world applications. This could enable quicker and more efficient quality control without the need for destructive testing. However, it is important to note that while the correlation is robust, variations in the microstructure, especially with higher FA contents, may introduce discrepancies in some cases. For example, the slower reaction of FA may cause variations in material uniformity, potentially affecting the relationship between UPV and CS in some high-FA mixes.

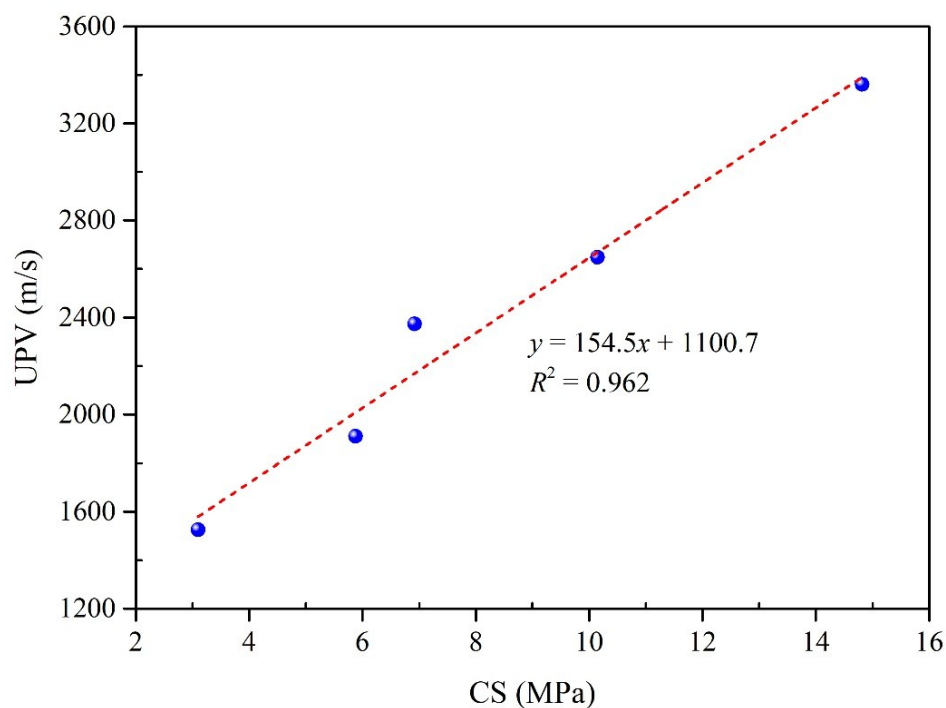


Fig. 7. Correlation between UPV and CS of GB samples

3.3. Electrical resistance

The ER values for the GB samples demonstrated a clear inverse relationship with the FA content, as shown in Fig. 8. As the FA replacement percentage increased, the electrical resistance significantly decreased, indicating a rise in the porosity and permeability of the material. The control mix (0% FA) exhibited the highest ER value of 18.3 kΩ.cm, which reflects the relatively dense structure of the material, with fewer interconnected pores and limited ion movement. In contrast, as FA

content increased, the ER values declined steadily, confirming that FA's inclusion alters the material's microstructure, making it more porous and less resistant to electrical flow. At 30% FA replacement, the ER dropped to 9.2 kΩ.cm, representing a 49.5% reduction from the control mix. This significant decrease in electrical resistance can be explained by the fact that FA particles have a greater surface area and porosity compared to cement. When added to the mixture, FA particles tend to create additional void spaces, increasing

the overall permeability of the material. This trend is consistent with the general understanding that higher porosity in construction materials leads to reduced ER, as the pores provide pathways for ions to move through.

Further increases in FA content led to even more significant reductions in ER. For the 50% FA mix, the ER value was reduced to 7.3 kΩ.cm, which represents a 60.1% decrease compared to the control. Similarly, the 70% FA mix had an ER of 5.9 kΩ.cm (67.7% reduction), and the 85% FA mix exhibited the lowest ER value of 5.1 kΩ.cm, corresponding to a 72.1% decrease from the control. This progressive reduction in ER with increasing FA content highlights the continued influence of FA on the porosity and water

absorption capacity of the bricks. As the FA content rises, the overall density of the material decreases, leading to more interconnected pores and thus greater ion conductivity through the material, which reduces ER. This observation was in good agreement with lower CS and UPV values in the GB samples, as discussed in Sections 3.1 and 3.2. The decreased ER values also suggest that higher FA mixes will likely have higher water absorption rates, which can affect the long-term durability and performance of the material, particularly in environments subject to moisture fluctuation. While higher porosity may be beneficial for applications requiring greater permeability, it may negatively impact the material's resistance to environmental degradation and moisture infiltration.

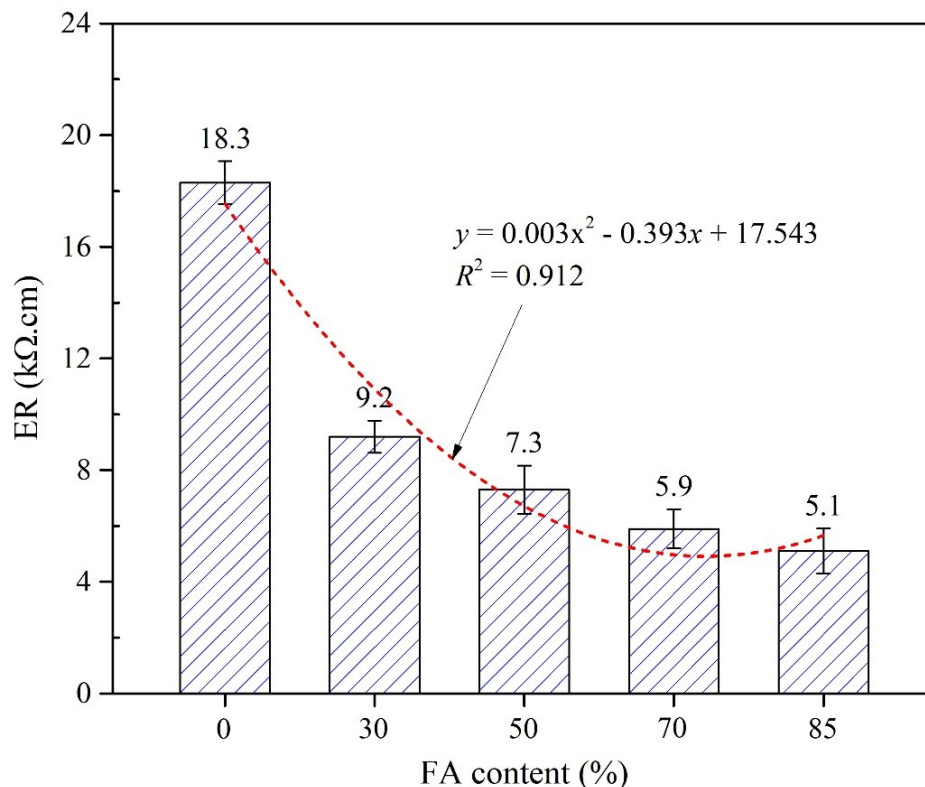


Fig. 8. ER of GB samples

3.4. Thermal conductivity

The TC values of the GB samples were measured to assess the impact of FA replacement on the heat transfer properties of the material. As shown in Fig. 9, the TC decreased as the FA content increased, reflecting a trend towards lower TC with higher levels of FA. The control mix (0% FA) exhibited the highest TC of 0.69 W/mK, which

gradually reduced with increasing FA content, indicating a decrease in heat conduction properties due to the physical and chemical characteristics of FA. At 30% FA replacement, the TC dropped to 0.51 W/mK, representing a 26.1% decrease compared to the control mix. The reduction in TC can be attributed to the lower density and increased porosity introduced by the addition of FA.

FA has a low TC itself, and when incorporated into the mix, it creates more voids and irregularities in the structure, reducing the overall ability of the material to conduct heat. As the FA content increases, the material's capacity to transfer heat diminishes, which is beneficial for applications requiring insulation properties. Further increases in FA content led to a more pronounced reduction in TC. For the 50% FA mix, the TC dropped to 0.45 W/mK, a 34.8% reduction from the control mix. At 70% FA replacement, the TC decreased further to 0.37 W/mK, representing a 46.4% reduction compared to the control. Finally, the 85% FA mix exhibited the lowest TC value of 0.29 W/mK, which is a 57.9% decrease from the original mix. This consistent decline in TC is a direct result of the increasing porosity and lower density associated with higher levels of FA. The higher FA content contributes to a more porous microstructure, which hinders the passage of heat through the material, making it a more effective insulator. These trends are consistent with previous studies, which have

reported that materials with higher porosity tend to have lower TC due to the increased air voids that act as thermal insulators [41]. These results are also consistent with the results of CS, UPV, and ER reported in previous sections. The lower TC of the FA-based mixes is advantageous for applications where insulation is a key factor, such as in energy-efficient buildings, where reducing heat transfer can contribute to better temperature control and lower energy consumption.

From a practical standpoint, the decrease in TC with higher FA content is beneficial for sustainability and energy efficiency. For example, the 85% FA mix (with the lowest TC value of 0.29 W/mK) could be an ideal candidate for non-load-bearing walls or insulation applications where heat retention and energy efficiency are crucial. On the other hand, the control mix (0% FA), with its higher TC of 0.69 W/mK, may be better suited for applications where heat conduction is desirable, such as in structural components exposed to varying temperature conditions.

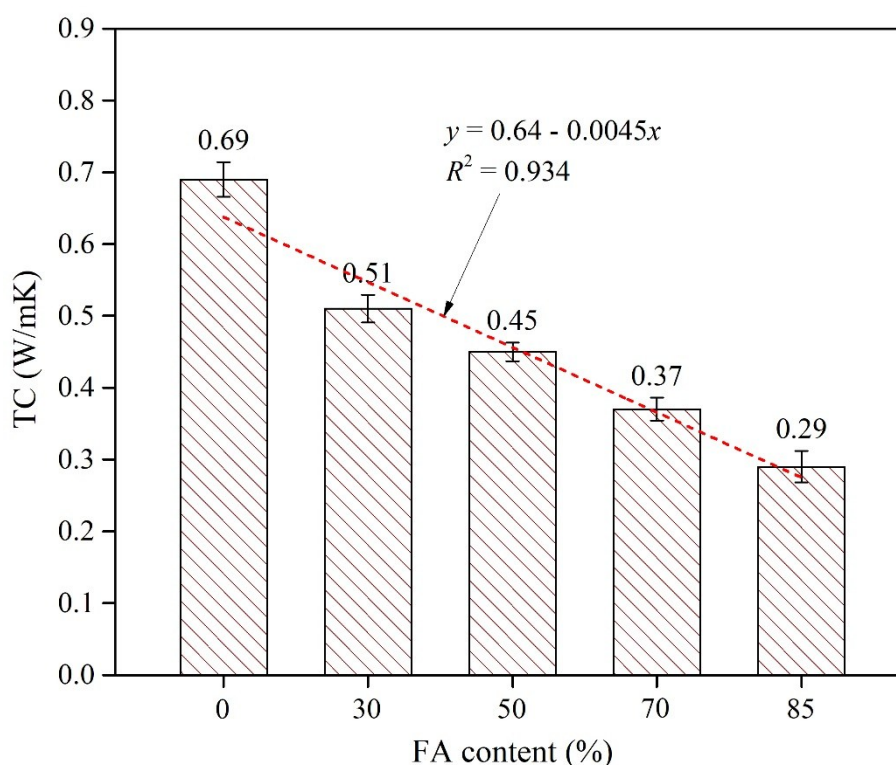


Fig. 9. TC of GB samples

3.5. SEM observations

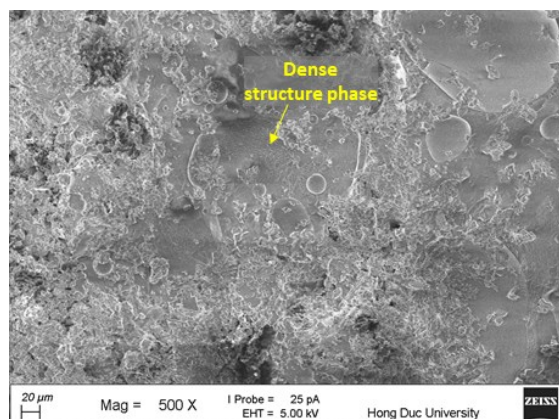
The SEM morphologies of the GB samples at various FA replacement levels are shown in Fig.

10. The SEM images reveal significant changes in the microstructure of the GB samples as the FA content increases, with noticeable effects on

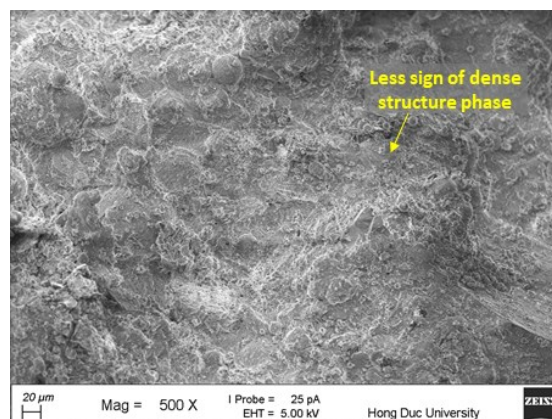
particle packing, porosity, and the overall compactness of the material. At MFA00 (0% FA), Fig. 10(a) shows a relatively dense structure with minimal visible porosity. The cement particles are well-formed, and the microstructure appears compact, indicating a well-hydrated cement matrix that contributes to the material's high strength and lower permeability. The particles are more tightly packed, and fewer air voids are visible, which is typical for mixtures with higher cement content. MFA30 (30% FA), shown in Fig. 10(b), demonstrates an increase in porosity compared to MFA00. While the microstructure still appears relatively cohesive, the presence of FA particles introduces more voids and irregularities in the matrix. These voids are likely due to the slower pozzolanic reaction of FA, which reduces the overall compactness of the material in the early stages of hydration. The inclusion of FA helps to reduce the overall density of the GB bricks, contributing to lower compressive strength and increased permeability, but it also brings sustainable benefits by utilizing a waste product. With MFA50 (50% FA) (Fig. 10(c)), the porosity becomes more pronounced. The microstructure shows larger and more interconnected voids, which can be seen as dark spaces between the particles. This is a direct result of higher FA content, which disrupts the material's density, leading to a more porous and less cohesive structure. While the increased porosity improves the material's insulation properties (as discussed in Section 3.4),

it contributes to a further reduction in the mechanical strength of the material. The FA particles appear less reactive compared to cement particles, further delaying the material's strength development. For MFA70 (70% FA) (Fig. 10(d)) and MFA85 (85% FA) (Fig. 10(e)), the increase in porosity is even more evident. The microstructure of MFA70 and MFA85 exhibits significant voids and an almost sponge-like appearance, indicating a substantial decrease in the material's compactness. The high FA content appears to inhibit the formation of a strong cementitious matrix, leading to the development of large, interconnected pores. These structural features are consistent with the observed reduction in CS (Section 3.1), UPV (Section 3.2), and ER (Section 3.3), as the increased voids allow for easier movement of ions and reduce the material's ability to withstand mechanical stresses.

Overall, the SEM observations confirm the trend of increasing porosity and decreasing microstructural compactness with higher FA content. While the inclusion of FA provides environmental benefits, including reduced CO₂ emissions from cement production and the utilization of waste material, it also compromises the mechanical properties of the GB. This trade-off between sustainability and material performance is particularly evident in the higher FA mixes (MFA50, MFA70, and MFA85), which show significant reductions in strength and resistance.

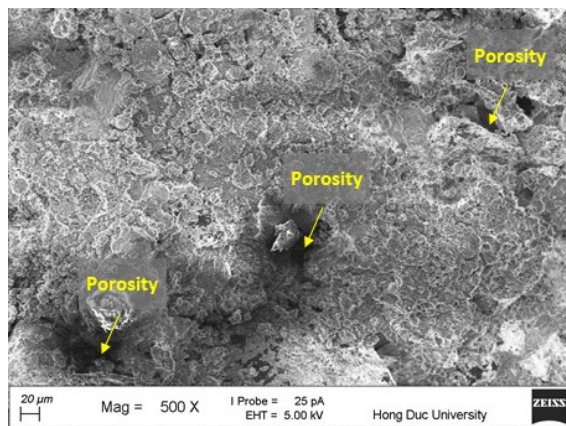


(a) MFA00

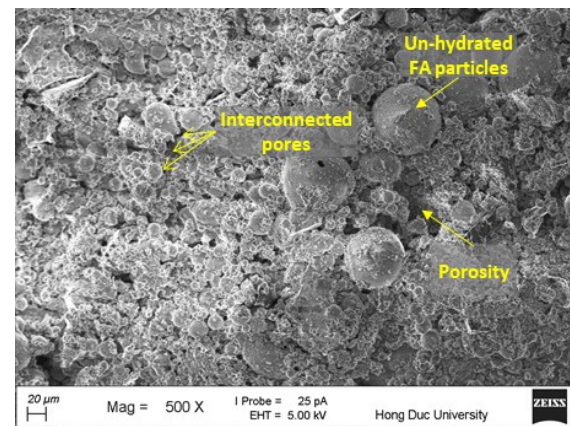


(b) MFA30

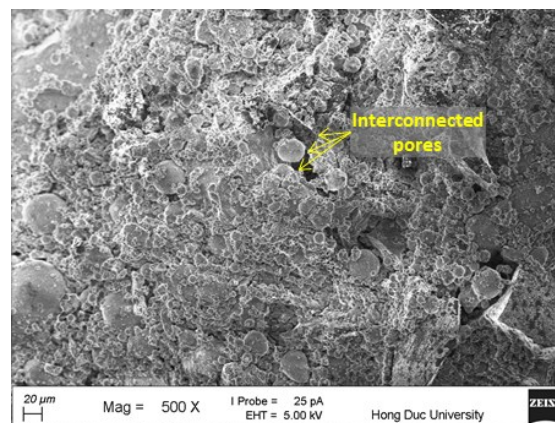
Fig. 10. SEM morphologies of GB samples at 28 days



(c) MFA50



(d) MFA70



(e) MFA85

Fig. 10. (continued)

3.6. XRD analysis

Fig. 11 presents the XRD patterns of the 28-day GB samples with varying FA content. The XRD analysis was used to identify the mineralogical composition of the samples, focusing on the presence of key crystalline phases, which include alite (A), belite (B), mulite (M), and quartz (Q). The XRD pattern of the 0% FA specimen (black line) shows distinct peaks corresponding to A and B, which are common phases in Portland cement. Alite, in particular, is associated with high early strength, while B is present in lower amounts and contributes to long-term strength development. Additionally, the presence of M and Q indicates the crystalline phases present in the cement matrix and any residual minerals. The control mix shows strong peaks for these phases, confirming the crystalline structure of the cement-based matrix with minimal disruption from other components. As FA content increases, there is a slight shift in the XRD patterns. At MFA30 (30% FA) (red line), the

pattern begins to show the influence of FA, with a slight reduction in the intensity of the A and B peaks. The peaks corresponding to Q become more prominent, reflecting the crystalline nature of FA, which primarily consists of amorphous silica and alumina but also contains crystalline Q. This shift in the XRD pattern suggests that the increasing presence of FA disrupts the traditional cement matrix, reducing the crystallinity and strength development associated with A while introducing more Q into the structure. For MFA50 (50% FA) (blue line), the A and B peaks become further diminished, and the Q peaks continue to increase in intensity. This trend indicates that the high FA content further reduces the cement's ability to develop a strong, dense structure, as FA's pozzolanic reaction is slower than that of cement. The increased presence of M in the mix is likely due to the FA reacting with lime over time, although at this stage, the material is still in a less reactive phase compared to fully hydrated cement. For

MFA70 (70% FA, magenta line) and MFA85 (85% FA, green line), the XRD patterns show even weaker peaks for A and B, with the Q peaks becoming more dominant. The presence of M is still visible, but the overall intensity of the diffraction peaks is much lower. These changes reflect a highly disrupted matrix due to the dominance of Q and the absence of sufficient cementitious material to fully react and hydrate. At these higher FA levels, the mix becomes increasingly amorphous, with FA contributing mainly to the long-term pozzolanic reaction rather than participating in the initial

formation of crystalline phases like A.

In summary, the higher FA mixes (MFA70 and MFA85) exhibit a less crystalline and more amorphous matrix, indicating the slower pozzolanic reaction of FA and the resulting reduced short-term performance of the material. This trend is consistent with the observed reductions in compressive strength and electrical resistance at higher FA contents. These findings underline the importance of optimizing FA content to balance sustainability with the mechanical properties of green building bricks.

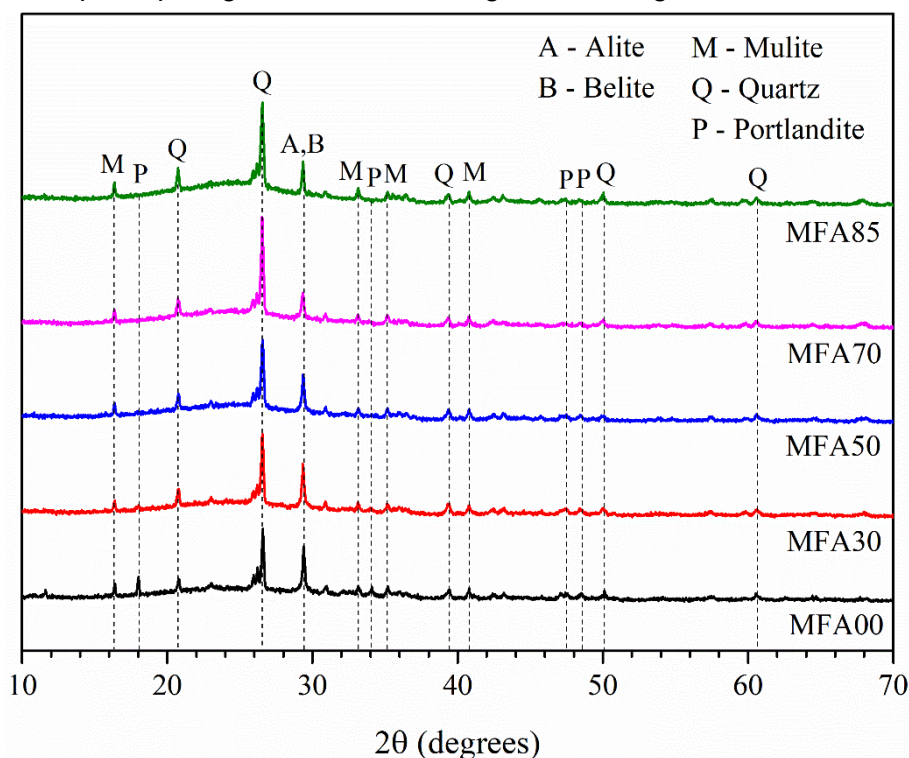


Fig. 11. XRD patterns of GB samples

4. Conclusion

This study highlights the potential of utilizing both FA and BA in GB production as a sustainable alternative to conventional materials. The findings provide new insights into the effects of FA replacement levels on the mechanical, physical, and microstructural properties of GB, thereby addressing a critical research gap as aforementioned. Moreover, by demonstrating the feasibility of coal combustion ashes in GB manufacturing, this investigation contributes to reducing the environmental footprint of coal combustion and supports the development of

greener, more sustainable building products for the construction industry. The experimental findings lead to the following conclusions:

- The CS of the GB samples decreased with increasing FA content. At 28 days, the control mix (MFA00) showed the highest CS of 14.82 MPa, while the MFA30 mix (30% FA) had a CS of 10.15 MPa, a reduction of 31.5%. Higher FA contents resulted in more significant reductions, with MFA50 (50% FA) showing a 53.3% reduction (6.92 MPa), MFA70 (70% FA) a 60.4% reduction (5.88 MPa), and MFA85 (85% FA) a 79.1% reduction (3.1 MPa). These results suggest that 30% FA provides

a balance between sustainability and performance, while higher FA levels compromise early-stage strength.

- The UPV followed a similar pattern, indicating reduced material density and quality with higher FA content. At 28 days, MFA00 had the highest UPV of 3360 m/s, and MFA30 showed a 21.3% reduction (2648 m/s). MFA50 (50% FA) showed 30.5% lower UPV (2374 m/s), MFA70 (70% FA) 43% lower (1910 m/s), and MFA85 (85% FA) 54.5% lower (1526 m/s). These reductions confirm that increasing FA leads to a less dense and more porous structure, especially in higher FA mixes.

- ER also decreased with increasing FA content. MFA00 exhibited the highest ER of 18.3 k Ω .cm, while MFA30 showed a 49.5% decrease (9.2 k Ω .cm). For higher FA mixes, ER values dropped progressively: MFA50 (60% reduction), MFA70 (67.7% reduction), and MFA85 (72.1% reduction). This trend highlights the increased porosity and permeability in the FA-based bricks, which allow for greater ion movement.

- The TC decreased as FA content increased, with MFA00 having the highest TC of 0.69 W/mK. The MFA30 mix showed a 26.1% reduction (0.51 W/mK), and the MFA50 showed a 34.8% reduction (0.45 W/mK). Higher FA contents resulted in even more significant reductions, with MFA85 exhibiting the lowest TC of 0.29 W/mK (57.9% reduction). These results indicate improved insulation properties in higher FA mixes, beneficial for energy-efficient applications.

- SEM and XRD analyses confirmed that higher FA content increases porosity and reduces the crystallinity of the material. The SEM images revealed unhydrated FA particles in the higher FA mixes, which contributed to reduced early-stage strength development. The XRD patterns showed a decrease in crystalline phases such as A and B, replaced by Q, a primary component of FA. The microstructure analysis further supports the findings of the mechanical performance of the GB samples, as poor microstructure was associated

with lower CS, UPV, and ER values.

- This study found that 30% FA replacement offers a promising solution for sustainable GB production, balancing environmental benefits and material performance, and meeting the target strength of ≥ 7.5 MPa for common use in a non-loading bearing wall construction. FA contents above 50% significantly affect both early and long-term performance, making them more suitable for other uses where long-term durability is prioritized.

Although the incorporation of FA led to reduced technical properties of the GB, this outcome remains both scientifically and practically meaningful. It underscores the inherent limitations of FA as a sole replacement, offering critical insights for optimizing its dosage in GB formulations. Moreover, the results highlight the trade-off between performance and environmental benefits, since FA use significantly lowers cement demand and the environmental footprint of the final products. Importantly, the findings emphasize the need to balance mechanical performance with sustainability in GB design, thereby advancing knowledge on coal combustion ash utilization and informing practical strategies for greener construction materials. However, this study has not analyzed the environmental impact of the use of FA and BA in GB. Therefore, future studies will evaluate the sustainability of these green building bricks using FA and BA.

References

- [1] Y. Zheng, X. Xi, H. Liu, C. Du, H. Lu. (2024). A review: Enhanced performance of recycled cement and CO₂ emission reduction effects through thermal activation and nanosilica incorporation. *Construction and Building Materials*, 422, 135763. <https://doi.org/10.1016/j.conbuildmat.2024.135763>
- [2] L.S. Ho, L.V. Quang, D.-T.V. Pham, T.-P. Huynh. (2025). Strength development and microstructural characterization of eco-cement paste with high-volume fly ash. *Results in Engineering*, 26, 105013.

- <https://doi.org/10.1016/j.rineng.2025.105013>
- [3] L.S. Ho, T.-P. Huynh. (2023). Long-term mechanical properties and durability of high-strength concrete containing high-volume local fly ash as a partial cement substitution. *Results in Engineering*, 18, 101113. <https://doi.org/10.1016/j.rineng.2023.101113>
- [4] S. Curpen, N. Teutsch, K. Kovler, S. Spatari. (2023). Evaluating life cycle environmental impacts of coal fly ash utilization in embankment versus sand and landfilling. *Journal of Cleaner Production*, 385, 135402. <https://doi.org/10.1016/j.jclepro.2022.135402>
- [5] M.I. Mostazid, Y. Sakai. (2023). Low-carbon footprint approach to produce recycled compacted concrete. *Ceramics International*, 49(13), 22219-22231. <https://doi.org/10.1016/j.ceramint.2023.04.052>
- [6] V.Q. Dang, V.N. Chau, N.T. Sang, P.H. Thuc, L.S. Ho. (2025). Mechanical properties and durability of concrete containing fly ash and GGBS for marine environment: A comprehensive study from laboratory perspective. *Proceedings of the Institution of Mechanical Engineers, Part L: Journal of Materials: Design and Applications*, 14644207251317612. <https://doi.org/10.1177/14644207251317612>
- [7] S. Nguyen, Q. Thai, L.S. Ho. (2021). Properties of fine-grained concrete containing fly ash and bottom ash. *Magazine of Civil Engineering*, 107(7), 10711. <https://doi.org/10.34910/MCE.107.11>
- [8] H.T. Le, S.T. Nguyen, H.-M. Ludwig. (2014). A study on high performance fine-grained concrete containing rice husk ash. *International Journal of Concrete Structures and Materials*, 8, 301-307. <https://doi.org/10.1007/s40069-014-0078-z>
- [9] Decision No. 1208/QĐ-TTg (2011). The national electricity development plan for the period 2011-2020 has a vision to 2030, the Prime Minister, Vietnam (In Vietnamese).
- [10] V.N. Chau, L.S. Ho, T.Q. Hoang, V.Q. Dang. (2024). Evaluating the suitability of incorporating sugarcane bagasse ash, polypropylene fibers, and sea sand-seawater in enhancing physico-mechanical properties of lightweight foamed concrete. *Science Progress*, 107(4), 00368504241306144. <https://doi.org/10.1177/00368504241306144>
- [11] P.T. Bui, L.S. Ho, J.-Y. Shi, T.-P. Huynh. (2023). Effect of low-calcium fly ash inclusion on long-term mechanical properties and durability of ground granulated blast furnace slag-based cement-free mortars. *Proceedings of the Institution of Mechanical Engineers, Part L: Journal of Materials: Design and Applications*, 238(4), 723-738. <https://doi.org/10.1177/14644207231196682>
- [12] L.S. Ho, B.-J. Jhang, C.-L. Hwang, T.-P. Huynh. (2022). Development and characterization of a controlled low-strength material produced using a ternary mixture of Portland cement, fly ash, and waste water treatment sludge. *Journal of Cleaner Production*, 356, 131899. <https://doi.org/10.1016/j.jclepro.2022.131899>
- [13] M. Adamu, P. Trabanpruek, P. Jongvivatsakul, S. Likitlersuang, M. Iwanami. (2021). Mechanical performance and optimization of high-volume fly ash concrete containing plastic wastes and graphene nanoplatelets using response surface methodology. *Construction and Building Materials*, 308, 125085. <https://doi.org/10.1016/j.conbuildmat.2021.125085>
- [14] G. Balotiya, A. Gaur, P. Somani, A. Sain. (2023). Investigating mechanical and durability aspects of concrete incorporating Wollastonite and bottom ash. *Materials Today: Proceedings*, S2214785323034284. <https://doi.org/10.1016/j.matpr.2023.06.048>
- [15] Z. Bian, Y. Huang, J.-X. Lu, G. Ou, S. Yang, C.S. Poon. (2023). Development of self-foaming cold-bonded lightweight aggregates from waste glass powder and incineration

- bottom ash for lightweight concrete. *Journal of Cleaner Production*, 428, 139424. <https://doi.org/10.1016/j.jclepro.2023.139424>
- [16] C.C. Ban, T.L. Ee, M. Ramli, H.B.M. Akil, K.H. Mo. (2022). Properties and microstructure of lime kiln dust activated slag-fly ash mortar. *Construction and Building Materials*, 347, 128518. <https://doi.org/10.1016/j.conbuildmat.2022.128518>
- [17] N.V. Tuan, N.N. Lam, N.C. Thang. (2018). Study on the influence of some technological parameters on the compressive strength of concrete bricks. *Journal of Science and Technology in Civil Engineering*, 12(2), 80-85. (in Vietnamese). [https://doi.org/10.31814/stce.nuce2018-12\(2\)-12](https://doi.org/10.31814/stce.nuce2018-12(2)-12)
- [18] Decision No. 1469/QĐ-TTg (2014). Approving the master plan for the development of Vietnam's construction materials to 2020 and vision to 2030, the Prime Minister, Vietnam. (in Vietnamese).
- [19] Directive No. 10/CT-TTg (2012). Increasing the use of unburnt construction materials and limiting the production and use of burnt clay bricks, the Prime Minister, Vietnam. (in Vietnamese).
- [20] Decree 24a/2016/NĐ-CP (2016). Management of construction materials, including encouragement of the development of unburnt construction materials, Vietnam Government. (in Vietnamese).
- [21] Decision No. 567/QĐ-TTg (2010). Approving the program for developing non-fired construction materials until 2020, the Prime Minister, Vietnam. (in Vietnamese).
- [22] M.I.-Hassan, M. Daud, K. Rashid, F.K. Alqahtani, I. Zafar, U. Batool. (2024). Development and sustainability assessment of red mud-based green bricks: Techno-economic and environmental performance. *Journal of Building Engineering*, 95, 110350. <https://doi.org/10.1016/j.jobbe.2024.110350>
- [23] C. Wang, J. Zhao, X. Zhao, R. Zhang, et al. (2025). Improving the applicability of green recycled aggregate permeable brick through target porosity and waste glass. *Construction and Building Materials*, 475, 141112. <https://doi.org/10.1016/j.conbuildmat.2025.141112>
- [24] M. Jothilingam, V. Preethi, P.S. Chandana, G. Janardhanan. (2023). Fabrication of sustainable green bricks by the effective utilization of tannery sludge as main additive. *Structures*, 48, 182-194. <https://doi.org/10.1016/j.istruc.2022.12.057>
- [25] A.N.-Hassani, H. Vashaghian, R. Hodges, L. Zhang. (2022). Production of green bricks from low-reactive copper mine tailings: Chemical and mechanical aspects. *Construction and Building Materials*, 324, 126695. <https://doi.org/10.1016/j.conbuildmat.2022.126695>
- [26] Q. Cai, P. Li, J. Luo, J. Feng, et al. (2023). Production of green autoclaved bricks from waste quarry sludge: Mechanical and microstructural aspects. *Construction and Building Materials*, 401, 132874. <https://doi.org/10.1016/j.conbuildmat.2023.132874>
- [27] S. Iftikhar, K. Rashid, E.U. Haq, I. Zafar, et al. (2020). Synthesis and characterization of sustainable geopolymer green clay bricks: An alternative to burnt clay brick. *Construction and Building Materials*, 259, 119659. <https://doi.org/10.1016/j.conbuildmat.2020.119659>
- [28] N.S.-Huy, L.T.T.-Tam, H.T.-Phuoc. (2020). Effects of NaOH concentrations on properties of the thermal power plant ashes-bricks by alkaline activation. *Journal of Wuhan University of Technology-Mater. Sci. Ed.*, 35, 131-139. <https://doi.org/10.1007/s11595-020-2236-2>
- [29] V.-D. Nguyen, S.-H. Ngo, T.-H. Mai, T.-P. Huynh. (2024). Durability and microstructure of high-strength mortar produced with high loss-

- on-ignition fly ash and silica fume. *Proceedings of the Third International Conference on Sustainable Civil Engineering and Architecture. ICSCEA 2023. Lecture Notes in Civil Engineering*, vol 442. Springer, Singapore, pp. 738-746.
https://doi.org/10.1007/978-981-99-7434-4_75
- [30] T.P. Huynh, V.-D. Nguyen, V.-L. Nguyen, T.-T. Le. (2024). Properties of unfired solid bricks produced primarily from thermal power plant fly ash and bottom ash. *CTU Journal of Innovation and Sustainable Development*, 16, 20-27.
<https://doi.org/10.22144/ctujoisd.2024.277>
- [31] T. Kien. (2023). Nghi Son 1 thermal power plant: Efforts to successfully implement the project's goals for treating ash, slag, and gypsum. (in Vietnamese).
- [32] Nguyen V.T. (2022). Nghi Son 1 Thermal Power Plant - Typical in ash, slag and gypsum consumption. Electricity industry database, 2022. (in Vietnamese).
- [33] H. Tung. (2022). Research on using waste rock mixed with coal ash of thermal power plants in the construction of highway embankments. *Journal of Science and Technology in Civil Engineering*, 16(3V), 1-6. (in Vietnamese).
[https://doi.org/10.31814/stce.huce\(nuce\)2022-16\(3V\)-01](https://doi.org/10.31814/stce.huce(nuce)2022-16(3V)-01)
- [34] L.D. Thi, L.T.T. Tam. (2021). Experimental investigation on the unfired building bricks produced from bottom ash and fly ash of Nghi Son coal power plant. *Hong Duc University Journal of Science*, 56, 95-102. (in Vietnamese).
- [35] N.T. Bang, N.T. Trung, D.H. Quan. (2019). Research on evaluating the quality of fly ash and blast furnace slag of thermal power and metallurgical plants in Vietnam. *J. Water Resour. Sci. Technol.*, 57, 27-39. (in Vietnamese).
- [36] Ministry of Science and Technology, Vietnam. (2016). TCVN 6477:2016, Concrete bricks. (in Vietnamese).
- [37] Ministry of Science and Technology, Vietnam. (2012). TCVN 9357:2012, Normal concrete - Nondestructive methods - Assessment of concrete quality using ultrasonic pulse velocity. (in Vietnamese).
- [38] T.-P. Huynh, D.-H. Vo, C.-L. Hwang. (2018). Engineering and durability properties of eco-friendly mortar using cement-free SRF binder. *Construction and Building Materials*, 160, 145-155.
<https://doi.org/10.1016/j.conbuildmat.2017.11.040>
- [39] S. Du, Q. Zhao, X. Shi. (2023). Quantification of the reaction degree of fly ash in blended cement systems. *Cement and Concrete Research*, 167, 107121.
<https://doi.org/10.1016/j.cemconres.2023.107121>
- [40] J. Chen, W. Zhu, Y. Shen, C. Fu, et al. (2023). Resource utilization of ultrasonic carbonated MSWI fly ash as cement aggregates: Compressive strength, heavy metal immobilization, and environmental-economic analysis. *Chemical Engineering Journal*, 472, 144860.
<https://doi.org/10.1016/j.cej.2023.144860>
- [41] T. Tang, L. Cai, K. You, M. Liu, W. Han. (2020). Effect of microwave pre-curing technology on carbide slag-fly ash autoclaved aerated concrete (CS-FAAAC): Porosity rough body formation, pore characteristics and hydration products. *Construction and Building Materials*, 263, 120112.
<https://doi.org/10.1016/j.conbuildmat.2020.120112>